

# Electronic properties of thienylene vinylene oligomers: synthesis and theoretical study

G. Neculqueo · V. Rojas Fuentes · A. López ·  
R. Matute · S. O. Vásquez · F. Martínez

Received: 27 October 2011 / Accepted: 14 February 2012 / Published online: 9 March 2012  
© Springer Science+Business Media, LLC 2012

**Abstract** (*E*)-1,2-bis(2-thienyl)vinylene (TV), (*E*)-1,2-bis(3-octyl-2-thienyl)vinylene (TOV), (*E*)-1,2-bis(3-(2-ethylhexyl)-2-thienyl)vinylene (T2EHV), and (*E*)-1,2-bis-[2,2'-bithienyl]vinylene (BTV) have been synthesized by a combination of formylation reaction and Mc Murry dimerization. UV–Vis spectra of BTV showed the longest wavelength absorption, TOV and T2EHV showed a bathochromic shift to the red compared with TV, due to an increment of delocalization of the conjugated  $\pi$ -system as the result of the weakening of the carbon–carbon double bonds of the thienyl rings due to the substitution of one hydrogen by the alkyl group. Based on optical data, the effect of linear and branched alkyl chain and extension of conjugation length on the electronic properties is discussed.  $^1\text{H}$ ,  $^{13}\text{C}$ -NMR, UV–Visible, Fluorescence data are discussed and theoretical DFT and TD-DFT calculations of ground state and excited states have been also considered in the analysis and explanation of results.

**Keywords** Thienylene vinylene · Oligomers · Optoelectronic · TD-DFT

## Introduction

In recent years the thienylene vinylene derivatives, formed from a combination of thiophene and the vinyl group, are known to have a delocalized  $\pi$  system, which is an important component for building electronic devices [1]. In addition, the incorporation of vinylene bonds between aromatic rings leads to an increment of the degree of planarity of the system and extend the conjugation length, reducing the steric hindrance in successive aromatic rings which is desirable for polymers to be used as electro-optical devices [2–5]. For instance, poly(thienylene vinylene) has a lower band gap than polythiophene [6–12] and can be regarded as a suitable material for semiconductor applications because of high flatness, high conductivity, and great potential mobility. [8, 13]

In this study, we compare the extension of conjugation length between thienylvinylene and bithienylvinylene and the effect of linear and branched alkyl chain on the electronic properties of thienylvinylene. Roncali et al. have reported the effect of increasing number of thiophene rings bridged by vinylene units and also compare the  $\alpha$  and  $\beta$  alkyl substituted thienylvinylene [5, 14]. They have concluded that alkyl substitution at  $\alpha$  position at the end of thiophene rings has little or none influence on the solubility and electronic properties, whereas mono or di-substitution at the  $\beta$  position of the thiophene rings enhances strongly the solubility. At the same time, spectroscopic and oxidation potential of thienyl-vinylene oligomers show expected bathochromic shift of  $\lambda_{\text{max}}$  and decrease of the HOMO–LUMO gap with extension of the conjugation length.

Theoretical approaches to calculate ground state and excited states properties have shown to be useful in this kind of systems and can yield interesting results on geometry aspects, localization-delocalization of the

G. Neculqueo · V. Rojas Fuentes · A. López ·  
S. O. Vásquez (✉) · F. Martínez (✉)  
Departamento de Ciencia de los Materiales, Facultad de Ciencias  
Físicas y Matemáticas, Universidad de Chile, Casilla,  
2777 Santiago Chile, Chile  
e-mail: svasqueza@ing.uchile.cl

F. Martínez  
e-mail: polimart@ing.uchile.cl

R. Matute  
Department of Chemistry and Biochemistry,  
University of California, Los Angeles, USA

$\pi$ -conjugated system and solvation effects [15], which are included in experimental electronic transitions. Recently, we have applied this approach to the study of the observed spectral features of 4,4'-bis(3-octylthienyl)biphenyl (OTBP) and 4,4'-bis(thienyl)biphenyl [16].

### Computational aspects

Calculations performed with Gaussian 03 and Gaussian 09 codes [17] consider optimization of the ground state geometry of TV, BTV, TOV, and T2EHV using the density functional theory (DFT) level of theory with the Becke, Lee, Yang and Parr B3LYP hybrid functional for exchange and correlation effects and the 6-31G+(d,p) basis set. Geometry optimizations were carried out in a two-step procedure: first as isolated gas phase molecules and subsequently we use the Tomasi's Polarized Continuum Model (PCM) to account for changes under the effect of the chloroform solvent.

The vertical  $S_0 \rightarrow S_1$  transition corresponding to absorption spectra of each of the four oligomers were resolved by time-dependent DFT (TD-DFT/B3LYP/6-31G+(d,p)) calculations [18]. Subsequent study of the geometry for the first excited singlet state is made by optimization using the TD-DFT/B3LYP/6-31G+(d,p) methodology implemented in G09 and finally data for the energies of the  $S_1 \rightarrow S_0$  emission were also obtained for TV, BTV, TOV, and T2EHV including solvent effects.

### Results and discussion

#### Absorption spectra

Figure 1 is the summary of the electronic absorption spectra of the four oligomers diluted in chloroform. The  $\lambda_{\max}$  absorption of (*E*)-1,2-di-(thiophene)vinylene (TV) at 344 nm is associated with the arrangement and delocalization of existing five conjugated double bonds in the molecule and its value is between the absorption wavelengths of 2,2'-bithiophene (300 nm and four conjugated bonds) and 2,2':5':2''-terthiophene (354 nm and six conjugated bonds), respectively, and consistent with the fact that a longer conjugation increases the value of wavelength [19]. The (*E*)-1,2-bis-[2,2'-bithienyl] vinylene (BTV),  $\lambda_{\max} = 434$  nm, which has nine conjugated double bonds, however absorbs 90 nm higher than TV ( $\lambda_{\max} = 344$  nm.) but compared with the quinquethiophene [2] having 10 conjugated double bonds, which absorbs at 416 nm, exhibits a higher bathochromic shift. This apparent contradiction, lower number of conjugated bonds and higher  $\lambda_{\max}$  than an analogous compound with higher number of  $\pi$ -delocalized bonds can be explained due to greater

rigidity of the structure as a result of the introduction of the vinylene unit in the structure, which reduce the steric interactions between the aromatic rings and extend the conjugation [2, 5, 14, 20], so it would produce a greater planarity and electron delocalization of  $\pi$  electrons. This effect would be even more pronounced when comparing the  $\lambda_{\max}$  of terthienyl vinylene, which absorbs at 462 nm (data not reported) with sexithiophene which absorbs to 434 nm, identical to our BTV with only four thiophene rings. Now, taking into account the effect of linear (TOV) and branched alkyl chain (T2EHV) on the electronic spectra (Fig. 1), we observe again a bathochromic shift,  $\lambda_{\max}$  353 and 354 nm respect to the 344 nm of TV.

Theoretical calculations were performed using the true structures for the unsubstituted TV and BTV oligomers but simplified structures for the alkyl OTV and T2EHV substituted oligomers. In fact, in the last cases, the eight member alkyl chain was shortened to just a  $\text{CH}_2\text{-CH}_2\text{-CH}_2\text{-CH}_3$  chain for OTV and a  $\text{CH}_2\text{-CH-(CH}_3)_2$  branched chain for T2EHV. As the alkyl chains are somewhat flexible and have rotational freedom along the chain axis, the longest alkyl chain, the slower the convergence of the calculation. To maintain cpu times within reasonable figures we used this simplified structures for OTV and T2EHV, keeping in mind that this kind of treatment has already been tested in previous work [16].

Figure 2 show the optimal geometry obtained for the four oligomers in ground state and the atomic labels considered for the following analysis.

Conformational aspects of the four oligomers in electronic ground state show that they are similar in nature. The TV is the only structure that is completely planar in gas phase and remains unchanged under the solvent effect of the chloroform (see Table 1 for details). Bond lengths of the nine C–C bonds of the dithienyl-vinylene chain show

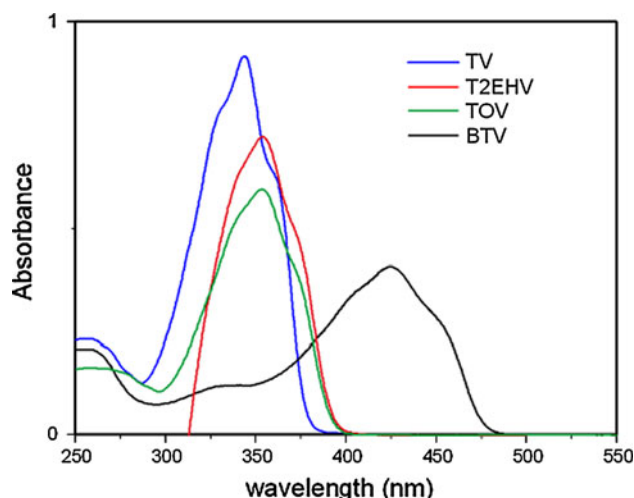
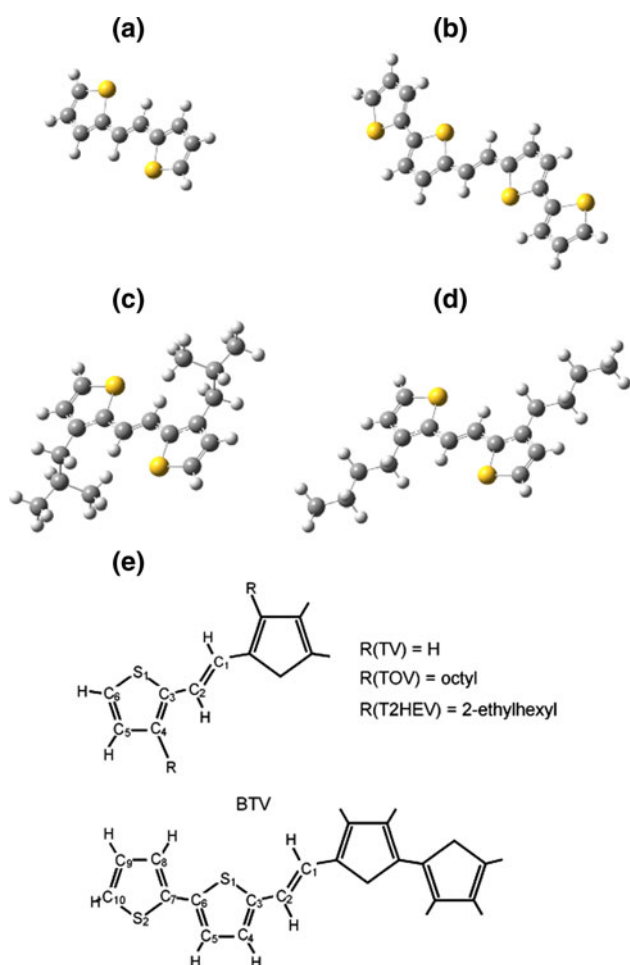


Fig. 1 Electronic absorption spectra of thienylvinylene oligomers



**Fig. 2** Geometries of the oligomers in the ground state: **a** TV, **b** BTV, **c** T2EHV and **d** TOV, **e** labels for carbon atoms in oligomers

**Table 1** Dihedral angles of the S–C–C–C central thienyl-vinyl sub-structure in the ground state and excited state geometry

	TV	T2EHV	TOV	BTV
$S_0$ ground state (gas phase)	0°	0.8°	2.5°	1.2°
$S_0$ ground state (solvent)	0°	1.7°	0.1°	0.9°
$S_1$ excited state (solvent)	0°	0.1°	0.0°	0.0°

A dielectric constant  $\epsilon = 4.9$  is considered for the chloroform solvent

an alternating shorter-longer pattern which is indicative that the conjugated  $\pi$  electronic system is not completely delocalized. This behavior is very similar both in gas phase and in solvent.

The central  $C_1$ – $C_2$  vinylic bond is the shortest of the series for every oligomer and, as a result of this, more double bond character (see Fig. 3a). Other carbon–carbon bonds show the expected zig-zag pattern of the single or double character of each specific pair bonded. Figure 4 includes the frontier molecular orbitals diagrams. In reference to the electronic densities of the HOMO of TV, the

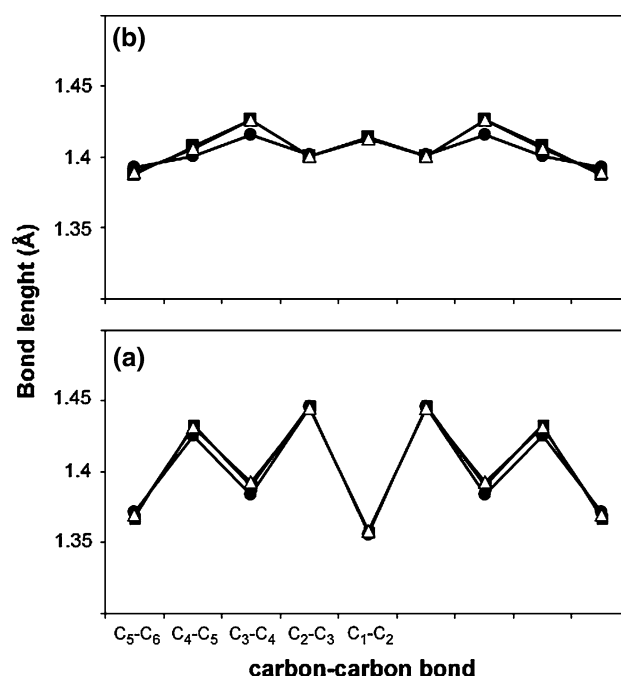


**Fig. 3** Bond lengths of the carbon–carbon conjugated  $\pi$ -system in: **a** the ground state and **b** the  $S_1$  excited state for TV (black dots), T2EHV (white triangles) and TOV (black squares)

bonding character between the  $C_1$ – $C_2$  and  $C_5$ – $C_6$  is clearly shown and we note that  $C_3$ – $C_4$  is distorted with the  $C_3$ – $S$  pair having a great contribution in the description of the electronic density of this part of the conjugated system. Comparison between the bond lengths and the HOMO molecular orbitals of TV and the models of the alkyl substituted oligomers T2EHV and TOV exhibit some differences in the electronic densities and geometry: the thienyl rings suffer from a small distortion due to the stretching of the  $C_3$ – $C_4$  and  $C_4$ – $C_5$  bond lengths as consequence of the substitution of hydrogen by the alkyl groups in the  $C_4$  carbon. Then, alkyl substitution induce a change in the electronic densities of the HOMO states by weakening the  $C_3$ – $C_4$  and  $C_4$ – $C_5$  bonds and delocalizing in some extent the electronic densities of T2EHV and TOV, as suggested by contour isosurfaces that are markedly greater in volume compared to TV. However, as the bond lengths of the central dithienyl-vinylene chain in TOV and T2EHV are almost identical (see Fig. 3a), we conclude that the only nature of the linear (in TOV) or branched (in T2EHV) chain structures makes no difference on the behavior of the electronic  $\pi$ -system of these alkyl substituted oligomers.

Dihedral angles of the S–C–C–C central thienyl-vinylene sub-structure are close to 0°. In gas phase, small differences between the four oligomers are observed and the decreasing order is dihedral (TOV) > dihedral (BTV) > dihedral (T2EHV) > dihedral (TV) = 0° (see

**Fig. 4** Frontier molecular orbitals of models of **a** TV, **b** T2EHV and **c** TOV oligomers (contour surface with isovalue = 0.015 for each figure)

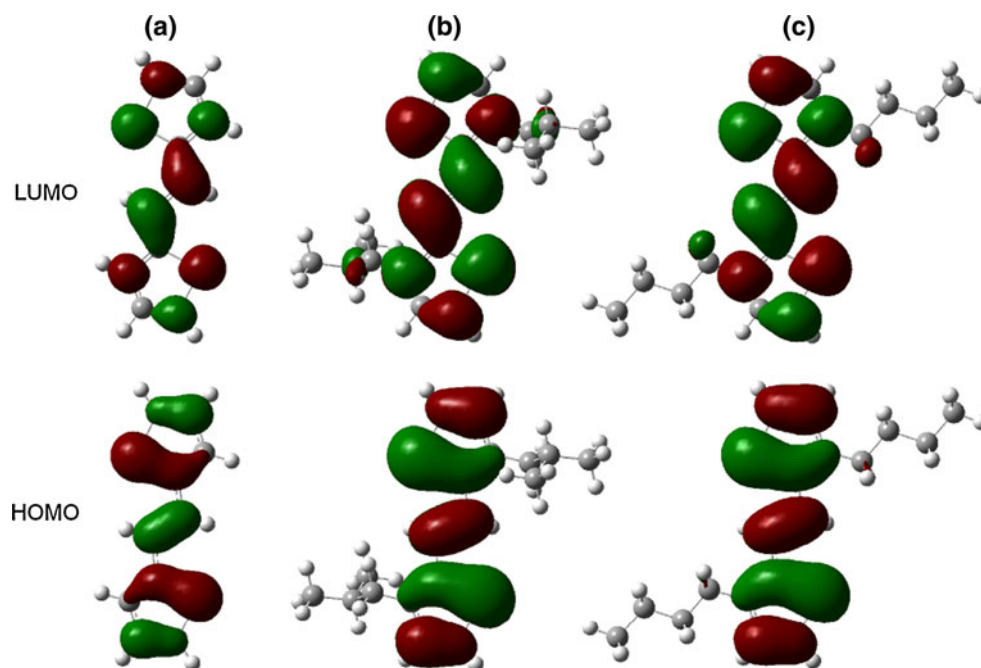


Table 1 for details). The effect of the substituents is observed in the case of TOV and T2EHV, causing a small distortion from planarity and that is somewhat bigger for TOV but difficult to interpret as the oligomer is almost planar as a whole. On the contrary T2EHV exhibit branched substituents located over and below the plane of the central thienyl-vinylene sub-structure but with a lower dihedral (see Fig. 2 for details). We postulate that the details and relative orientation of the ethylhexyl or octyl substituent chain with respect to the rings produce this unpredictable effect in the geometry of the lowest energy. For BTV the explanation is simple as the third and fourth thiophene rings added in both sizes of the TV induces twisting of the entire structure, a well known behavior already observed in oligothiophenes [21].

When we add the chloroform solvent effect into the calculations, TOV and BTV become more planar as expected considering a previous study [16] which interprets the effect of the solvent as a compression on the oligomer, action which results in an easier distortion along single bonds rather than more rigid structures such as double or triple bonds or carbon rings and making more planar structures. However, T2EHV does not follow this trend, because of the bulky 2-ethylhexyl groups which project over and under the almost planar central thienyl-vinylene and causing a non expected small increment on S–C–C–C dihedral of about 1 degree. A plausible explanation for this difference in the geometry optimizations might come from the fact that the compression exerted by the solvent could include a sort of lever action on the branched substituents, particularly due to steric hindrance between the CH<sub>3</sub> and the thienyl ring.

Vertical absorption transitions are then calculated using time-dependent DFT for the optimal geometries including

Tomasi's Polarized Continuum Model (PCM) and chloroform as the solvent. We do not expect an exact agreement between calculated and experimental wavelengths but the general trend is explained fairly well (see Table 2) and, in particular, figures for the vertical absorption of TV are in agreement to those reported by Meng et al. [22]. Differences on the  $S_0 \rightarrow S_1$  transition between TV and T2EHV and TOV can be attributed specifically to the alkyl substituents leading to an increment on delocalization of the  $\pi$ -cloud. There is also some electronic density that extends to the first member of the alkyl chain, an effect that is more important in TOV (Fig. 5) and that could explain its longer wavelength compared to T2EHV. In relation to TV, the red shifts in absorption are: 12.25 (10.0) nm for T2EHV, 25.59 (9.0) nm for TOV, and 119.79 (90) nm for BTV, where experimental values are in parenthesis. Table 3 also include very similar calculated oscillator strengths for the TV, T2EHV, and TOV trio, which means that the absorption spectra should have peaks of similar intensity. However, this could not be compared directly to experimental spectra in Fig. 1, as they were recorded at different concentration of the oligomers in chloroform.

The overestimated red shift for TOV seems to be the result of the optimum geometry found in the ground state which is more planar than the T2EHV oligomer. Although we have used shortened substituents, unreported preliminary results show that calculations with longer and more representative alkyl substituents do not change in a significant extent this picture for the ground state optimum geometry of both oligomers. Keeping in mind that the octyl groups have some extent of rotational freedom along the C–C bonds we postulate that less planar conformations of

TOV, due to slightly distorted linear substituents, could play an important role in lowering the calculated red shift of TOV at experimental conditions.

Having nine conjugated double bonds, BTV is in a different category and have the most pronounced red shift and longest wavelength of the family. Despite of the fact that it is in qualitative agreement to the sequence of UV–Vis experimental absorption maxima, a larger difference between calculated and experimental energies are readily observed: ( $E_{\text{exp}}/E_{\text{calc}} = 0.85$ ). This kind of disparity has already been observed for DFT calculations of an even longer oligomer: (tetra-2,5-thienylene-1,2-vinylene having eleven conjugated double bonds) [24] and is a proof of the limits of the methodology, at least under the basis set and the exchange–correlation functional choices considered in this study.

### Fluorescence analysis

For an excitation wavelength of 340 nm, the fluorescence spectrum of (*E*)-1,2-di-(2-thienyl) vinylene, have an emission signal at 402 nm, being greater than in the absorption transition and generating a shift of  $\lambda_{\text{max}}$  to higher values. This phenomenon is known as Stokes shift and is characteristic for such compounds and is commonly reported as a consequence of a more planar in the excited states. From the fluorescence spectra (Fig. 6) it can be observed that the T2EHV and TOV monomers with thiophene-vinylene substituent groups have the same emission wavelength at 417 nm suggesting a more planar S–C–C–C central thienylvinyl sub-structure and, therefore, less energy.

Optimization of geometry of the first excited electronic state reveals interesting changes for the family of compounds. Based on bond lengths, the dithienyl-vinylene chain in TV, TOV, and T2EHV is much more delocalized: C–C distances become very similar (around 1.4 Å) except for the C<sub>3</sub>–C<sub>4</sub> bond of T2EHV and TOV which are somewhat larger (see Fig. 3). For BTV delocalization is also evident in the central dithienyl-vinylene substructure (see Fig. 7a) and resulting in a pronounced delocalization of the  $\pi$ -electron cloud along the larger BTV molecule.

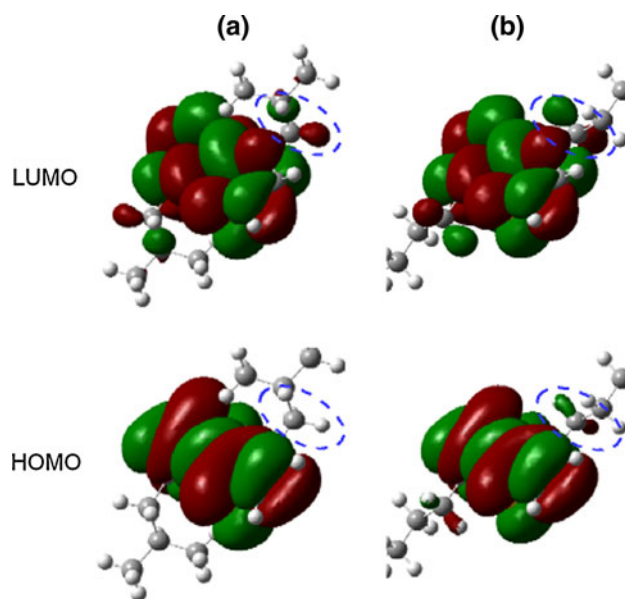


**Fig. 5** Detail of the frontier molecular orbitals of the **a** T2EHV and **b** TOV oligomers. The first CH<sub>2</sub> of the alkyl substituents has been highlighted (contour surface with isovalue = 0.012 for each figure)

Only the terminal C<sub>8</sub>–C<sub>9</sub> and C<sub>9</sub>–C<sub>10</sub> bonds remain almost unchanged in lengths and nature. In Fig. 4, the LUMO show that the C<sub>2</sub>–C<sub>3</sub> become the more bonding character of all the pairs, the C<sub>4</sub>–C<sub>5</sub> pair increase its electronic density and that the C<sub>5</sub>–C<sub>6</sub> bond (although shorter) have an electronic density clearly distorted to the C<sub>6</sub> position. All this details are consistent to a change from aromatic form (in the S<sub>0</sub> ground state) to a quinoid form (in the S<sub>1</sub> excited state) of TV and the alkyl substituted oligomers. From inspection of the changes in dihedral angles (Table 1) it is observed that the general criteria of more planar conformations for the excited state are fulfilled: TV, TOV, and BTV have central S–C–C–C dihedrals completely flat and T2EHV become almost planar. In the case of the T2EHV oligomer the tiny non zero dihedral angle is the result of the two combined movements which are not related to an increment on conjugation : (i) The sulfur atoms, which weaken their two S–C bonds, tend to move out of the

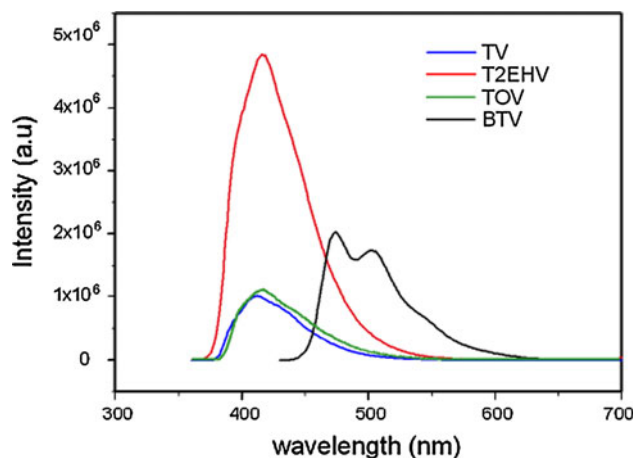
**Table 2** Absorption S<sub>0</sub> → S<sub>1</sub> vertical transition (ABS) and fluorescence S<sub>1</sub> → S<sub>0</sub> vertical transition (FL) energies, transition wavelengths, oscillator strengths, and Stokes shifts

	TV		T2EHV		TOV		BTV	
	ABS	FL	ABS	FL	ABS	FL	ABS	FL
Calculated $\Delta E$ (eV) ( $\lambda_{\text{max}}$ in nm)	3.445 (360.1)	952 (420)	3.332 (372.4)	2.824 (439)	3.216 (385.7)	2.75 (450.9)	2.585 (479.9)	2.237 (554.2)
Experimental $\Delta E$ (eV) ( $\lambda_{\text{max}}$ in nm)	3.607 (344)	3.086 (402)	3.505 (354)	2.975 (417)	3.515 (353)	2.975 (417)	2.859 (434)	2.64 (470)
$f_{\text{osc}}$ (a.u)	0.817	0.783	0.762	0.724	0.777	0.747	1.505	1.585

Calculated data include the effect of chloroform as solvent

**Table 3** Sulfur–carbon bond lengths (Å) in the ground state and excited state geometry, including chloroform solvent effect

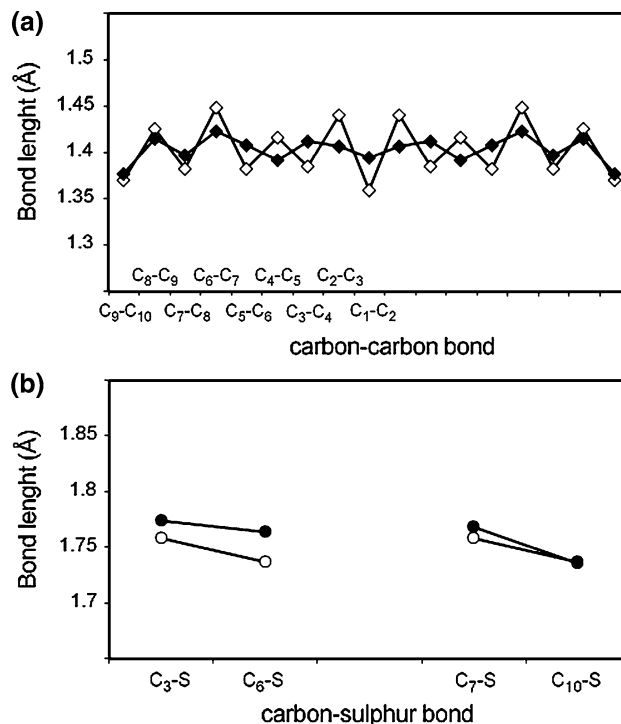
State	TV		T2EHV		TOV		BTV			
	S–C <sub>3</sub>	S–C <sub>6</sub>	S–C <sub>3</sub>	S–C <sub>6</sub>	S–C <sub>3</sub>	S–C <sub>6</sub>	S <sub>1</sub> –C <sub>3</sub>	S <sub>1</sub> –C <sub>6</sub>	S <sub>2</sub> –C <sub>7</sub>	S <sub>2</sub> –C <sub>10</sub>
S <sub>0</sub>	1.76	1.74	1.76	1.74	1.76	1.73	1.76	1.74	1.76	1.74
S <sub>1</sub>	1.79	1.73	1.79	1.73	1.79	1.73	1.77	1.76	1.77	1.74

**Fig. 6** Fluorescence spectra of thienylvinylene oligomers

thienyl ring and in the opposite direction of the bulky branched substituent which fill a volume outside the plane of the dithienyl-vinylene substructure and (ii) these alkyl groups tend to separate even more off the plane. This result warns over the need of a careful examination of all the geometric parameters when comparing ground versus excited electronic states.

Another interesting aspect is the change in sulfur–carbon bond length. Each thienyl ring have two different S–C lengths: S–C<sub>3</sub>, which is longer and facing the central HC=CH group and the S–C<sub>6</sub> a shorter bond located to the outside of the oligomer and less directly related to the conjugation. Not unexpectedly, these bond lengths are very similar for TV, TOV, T2EHV: about 1.76 and 1.74 Å, respectively, in ground state. When excited, the more delocalized  $\pi$ -system induces a weakness of the S–C<sub>3</sub> bond: they become longer (S–C<sub>3</sub>) and remains almost unchanged (S–C<sub>6</sub>) and with nodal planes in the S–C internuclear distance, keeping sulfur as electronic densities quasi isolated (see Fig. 4). Similar behavior is observed in BTV: stretching of the internal sulfur–carbon bonds and the external S–C<sub>10</sub> keeping its length (see Table 3).

Following a similar trend to the HOMO, electronic densities of T2EHV and TOV LUMOs are less spatially constrained and then more delocalized than TV. In these cases it is easy to observe also the existence of a small contribution on the alkyl substituents to the electronic densities, causing even more delocalization.

**Fig. 7** Bond lengths in BTV: **a** the carbon–carbon conjugated  $\pi$ -system and **b** the sulfur–carbon bond. In both cases, white dots or rhombs are for the S<sub>0</sub> ground state and black dots or rhombs for the S<sub>1</sub> excited state

Theoretical calculations on emission transitions consider a re-optimization of the geometry using TD-DFT/B3LYP//6-31G+(d,p) to the first excited singlet state and a subsequent calculation of the transition. TV energies of the S<sub>1</sub> → S<sub>0</sub> emission are in very good agreement to literature: 2.95 versus 2.98 eV [22].

Following a similar behavior to vertical absorption transition calculations, the S<sub>1</sub> → S<sub>0</sub> emissions also show the bathochromic effect due to the substitution of hydrogen with alkyl chains: taking the transition of TV as a reference, the red shifts in emission are: 19.0 (15.0) nm for T2EHV, 30.9 (15.0) nm for TOV, and 134.2 (68.0) nm for BTV, where experimental values are in parenthesis (see Table 2 for details).

Finally focusing on the TV, T2EHV, and TOV family, Stokes shifts between absorption–emission maxima can be obtained from Table 2. The shifts are in good agreement with experimental data (see Fig. 8) with differences lesser than 6% and is a complementary proof of the usefulness of this study.

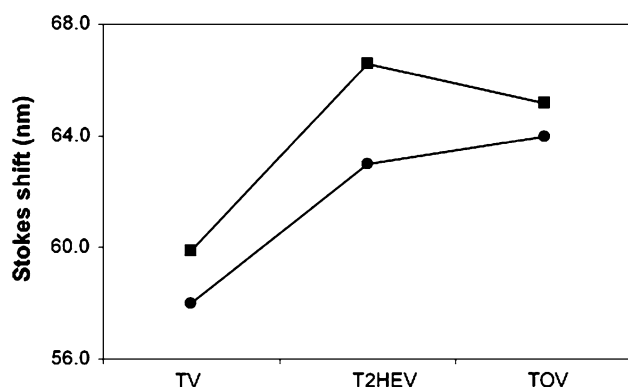


**Fig. 8** Stokes shift for the TV, T2EHV, and TOV family. *Black dots* represents experimental shifts, *black squares* are calculated shifts

## Conclusions

We have successfully prepared alkylthienyl oligomers. The UV–Vis absorption spectra of these compounds showed clear difference resulted from different band gap. Such differences were assigned to the different incorporating vinylene bonds between thiophene rings which lead to an increasing degree of coplanarity of the oligomer, as the vinylene bond reduces steric hindrance on successive aromatic rings.

From the theoretical viewpoint, structural changes and electronic densities of the ground and first excited electronic states are useful to explain the observed spectral changes in the TV, TOV, T2EHV, and BTV family of oligomeric entities. A first basic result is the geometry differences between both states, which show clearly the weakening of the double bonds of the central dithienyl-vinylene, based on the analysis of carbon–carbon bond lengths and planarization of the dihedral angles in the  $S_1$  excited state. These details are consistent to a change from aromatic form (in the  $S_0$  ground state) to a quinoid form (in the  $S_1$  excited state) of the oligomers. Considering the  $S_0$  ground state and related to TV, the alkyl substitution in the TOV and T2EHV duet induce an increment in the delocalization of the conjugated electronic  $\pi$ -system and results in a red shift of the absorption spectral features. As expected, the longer non-substituted BTV has an even bigger shift due to its longer conjugation length. However, the fact that the experimental very similar maxima (both in absorption and fluorescent vertical transitions) for TOV and T2EHV is not well explained by our calculations could be the consequence of the linear (TOV) or branched (T2EHV) alkyl substitution: the  $S_0$  ground state of TOV (in chloroform solvent) is more delocalized and almost perfectly planar as the lineal alkyl group are linear and coplanar to the central dithienyl-vinylene structure and leads to a calculated red shift bigger than the T2EHV oligomer, in which the branched alkyl substituents acts as levers and distorts in a small extent the central dithienyl-vinylene and under the solvent effect. We stress that we never expected an exact agreement between calculated and

experimental spectral features, that the results are in fairly well global agreement and that the apparent discrepancies could be searched improving the methodology. One possibility to be investigated is to make corrections correlating experimental data with calculated spectroscopic features of slightly distorted model structures of the stable conformers, in a similar way to the method used by Diliën et al. [23] to predict NMR chemical shifts assignments of poly(3-octylthienylene vinylene) polymerization defects. However, preliminary results on the change of the absorption/fluorescence peak maxima by distorting the geometry of the alkyl substituents does not produce significant enough shifts of the absorption/fluorescence features. The fact that Stokes shifts of the TV, T2EHV, TOV oligomers is reasonably well explained, although with a systematic overestimation between 2 and 6% points to the necessity of a further investigation with different correlation-exchange functionals or at a higher level of methodology (MP2, for instance) but is beyond the scope of this study. In the  $S_1$  excited electronic state, we observed that the delocalization of the electronic densities is even more marked than the  $S_0$  ground state, including a small contribution to the alkyl substituents to the electronic densities and the calculated fluorescent vertical transitions follow similar trends to the absorption transitions previously mentioned.

## Experimental section

### General information

All solvents were purchased from commercial sources and were distilled prior use, catalyst and reagents were used as received without further purification. Thin-layer chromatography (TLC) was performed using silica gel 60 F254 precoated plates.  $^1\text{H}$  and  $^{13}\text{C}$  NMR spectra were recorded on NMR spectrometer operating at 300 and 75.5 MHz, respectively. The  $^1\text{H}$  chemical shifts are reported in parts per million relative to tetramethylsilane. UV–Vis and fluorescence spectra were recorded on chloroform solution.

### Experimental procedure

#### 3-Octylthiophene (**1a**)

According to reported method of Kumada coupling [24]. A regioselective Grignard cross coupling reaction of octylbromide with 3-bromothiophene, catalyzed by  $\text{Ni}(\text{dppp})\text{Cl}_2$  (Nickel diphenylphosphino-propane) (**24**) give 22.6 g (73% yield) of **1a**; refractive index 1.4921; UV–Vis  $\lambda_{\text{max}}$  ( $\text{CHCl}_3$ ): 241 nm.

$^1\text{H}$ -NMR ( $\text{CDCl}_3$ , 400 MHz)  $\delta$ (ppm) 7.31 (dd, 1H,  $J = 3.0$  Hz,  $J = 4.9$  Hz); 7.01 (m, 2H); 2.72 (t, 2H,

$J = 7.7$  Hz); 1.72 (q, 2H); 1.37 (m, 10H); 0.99 (t, 3H,  $J = 6.8$  Hz);  $^{13}\text{C}$ -NMR ( $\text{CDCl}_3$ , 400 MHz):  $\delta$ (ppm) 143.6; 128.6; 125.3; 120.1; 32.1; 30.9; 30.7; 29.1; 29.7; 29.64; 23.0; 14.5.

### 3-(2-Ethylhexyl)thiophene (**1b**)

The procedure is same as above (1a) but in this case, 2-ethylhexyl bromide was used instead of octyl bromide. The product is a colorless liquid, was obtained with 65% yield, refractive index: 1.4877. Product weight: 20.1 g. Percentage yield: 65%, UV–Vis  $\lambda_{\text{max}}$  ( $\text{CHCl}_3$ ): 241 nm.

$^1\text{H}$ -NMR ( $\text{CDCl}_3$ , 400 MHz)  $\delta$ (ppm) 7.29 (m, 1H); 6.99 (m, 2H); 2.63 (d, 2H,  $J = 6.9$  Hz); 1.62 (tt, 1H,  $J = 6.3$  Hz,  $J = 12.4$  Hz); 1.36 (m, 8H); 0.94 (m, 6H).  $^{13}\text{C}$ -NMR  $\delta$ (ppm) ( $\text{CDCl}_3$ , 400 MHz): 142.0; 128.8; 124.8; 120.7; 40.5; 34.4; 33.0; 29.0; 25.7; 23.1; 14.2; 10.9.

### 3-Octyl-2-thiophenecarboxaldehyde (**2a**)

3 mL of phosphorus oxychloride (32 mmol) were added dropwise to a solution containing 5.6 g (0.028 mmol) of 3-octylthiophene and 2.5 mL DMF (0.032 mmol) in 10 mL of 1,2-dichloroethane at 0 °C. The solution was gradually brought to room temperature and refluxed overnight. The solution was cooled to room temperature and hydrolyzed with 100 mL of aqueous solution of sodium acetate. The solution was extracted with dichloromethane. The organic layer was washed with water, dried over anhydrous magnesium sulfate and concentrated under reduced pressure. The product was purified by column chromatography (silica gel, hexane/dichloromethane) to give a 5.73 g (89%) of light yellow oil. Refractive index: 1.5214 UV–Vis  $\lambda_{\text{max}}$  ( $\text{CHCl}_3$ ): 275 nm.

$^1\text{H}$ -NMR ( $\text{CDCl}_3$ , 400 MHz)  $\delta$ (ppm) 10.4 (s, 1H); 7.65 (d, 1H,  $J = 4.7$  Hz); 7.01 (d, 1H,  $J = 4.9$  Hz); 2.96 (t, 1H,  $J = 7.7$  Hz) 2.64 (t, 1H, 7.7 Hz); 1.67 (m, 2H); 1.26 (m, 10H); 0.88 (t, 3H,  $J = 6.6$  Hz);  $^{13}\text{C}$ -NMR ( $\text{CDCl}_3$ , 400 MHz)  $\delta$ (ppm); aldehyde 182.50; aromatics 153.13; 137.85; 134.6; 130.9; aliphatics 32.0; 31.7; 29.5; 29.5; 29.4; 28.7; 22.9; 14.3.

### 3-(2-Ethylhexyl)-2-thiophenecarboxaldehyde (**2b**)

The procedure is same as above (2a) but in this case, use 3-(2-ethylhexyl)thiophene instead of 3-octylthiophene. Yield 78%, yellow oil, refractive index: 1.5211. UV–Vis  $\lambda_{\text{max}}$  ( $\text{CHCl}_3$ ): 302 nm.

$^1\text{H}$ -NMR ( $\text{CDCl}_3$ , 400 MHz);  $\delta$ (ppm) 10.07 (s, 1H); 7.65 (d, 1H,  $J = 4.7$  Hz); 7.01 (d, 1H,  $J = 4.9$  Hz); 2.92 (d, 1H,  $J = 7.2$  Hz); 2.61 (d, 1H,  $J = 6.9$  Hz); 1.65 (dd, 1H,  $J = 6.0$  Hz); 1.31 (m, 8H); 0.92 (t, 6H,  $J = 7.3$  Hz);  $^{13}\text{C}$ -NMR ( $\text{CDCl}_3$ , 400 MHz):  $\delta$ (ppm) 182.4; 152.1; 137.6;

134.18; 131.3; 41.6; 34.2; 32.8; 28.8; 25.8; 23.0; 24.1; 10.8.

### (*E*)-1,2-Di-(3-octylthiophene)vinylene (**3a**)

To a solution of 4.48 g of 3-octyl-2-thiophenecarboxaldehyde in 75 mL of anhydrous THF is added 6.6 mL of titanium tetrachloride at  $-18$  °C. The mixture is stirred for half an hour at  $-18$  °C. To this solution were added 8.0 g of Zn powder in small portions for 10–15 min. The mixture was stirred for 30 min at  $-18$  °C and allowed to reach room temperature gradually, and then heated for 4 h at reflux. The mixture was cooled in an ice-water bath and 50 mL of aqueous solution of sodium carbonate 10% were added. Then, 200 mL of dichloromethane were added in portions of 50 mL and two layers mixture is stirred after being filtered. The dichloromethane layer is separated from the filtrate and washed with water until neutral pH. Later, dried with magnesium sulfate for 3 h and the solvent was filtered and evaporated, leaving an orange liquid, which is purified by column chromatography, eluting with hexane giving 2.00 g product (48% yield).

$^1\text{H}$ -NMR ( $\text{CDCl}_3$ , 400 MHz)  $\delta$ (ppm) 7.07 (d, 2H,  $J = 5.1$  Hz); 7.02 (s, 2H); 6.85 (d, 2H,  $J = 4.9$  Hz); 2.67 (t, 2H,  $J = 7.6$  Hz); 2.56 (t, 2H,  $J = 7.6$  Hz); 1.60 (m, 4H); 1.27 (m, 20H); 0.87 (t, 6H);  $^{13}\text{C}$ -RMN ( $\text{CDCl}_3$ , 400 MHz);  $\delta$ (ppm) 140.9; 136.5; 130.1; 122.7; 119.7; 32.1; 31.2; 29.7; 29.61; 29.5; 28.7; 22.9; 14.4.

### (*E*)-1,2-Di-(3-(2-ethylhexyl)thienyl)vinylene (**3b**)

The procedure is same as 3a, but in this case 3-(2-ethylhexyl)-2-thiophenecarboxaldehyde was used instead of 3-octyl-2-thiophene carboxaldehyde. Product weight: 1.67 g (40% yield).

$^1\text{H}$ -RMN (400 MHz,  $\text{CDCl}_3$ , ppm);  $\delta$ (ppm) 7.30 (s, 2H); 7.10 (d, 2H); 6.86 (d, 2H); 2.62 (d, 4H); 1.57 (q, 2H); 1.35 (m, 16H); 0.95 (t, 12H).

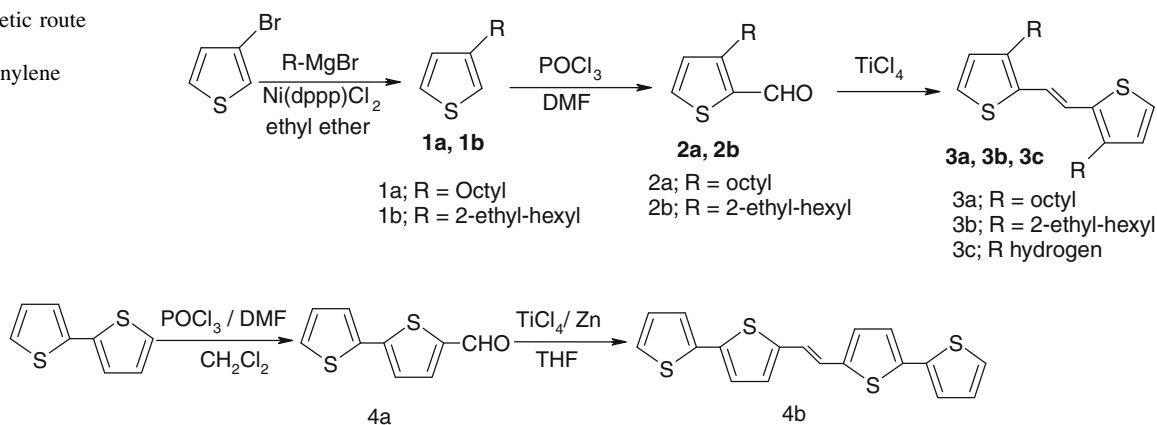
$^{13}\text{C}$ -RMN (400 MHz,  $\text{CDCl}_3$ );  $\delta$ (ppm) aromatics: 139.0; 137.0; 130.5; 122.4; 120.2; aliphatics: 40.8; 34.6; 32.3; 29.0; 25.8; 22.9; 14.2; 10.9.

### (*E*)-1,2-Di-(2-thienyl)vinylene (**3c**)

The procedure is same as 3a, but in this case thiophene-2-carboxaldehyde was used instead of 3-octyl-2-thiophene-carboxaldehyde (83.9% yield) [25]

$^1\text{H}$ -NMR (400 MHz,  $\text{CDCl}_3$ ):  $\delta$ (ppm) 6.96–6.99, (dd, 2H), 7.02–7.04 (d, 2H), 7.05 (s, 2H,  $-\text{CH} = \text{CH}-$ ), 7.15–7.18 (d, 2H).

$^{13}\text{C}$ -RMN (400 MHz,  $\text{CDCl}_3$ );  $\delta$ (ppm) aromatics: 144.4; 128.1; 127.0; 125.88; 124.3 (Scheme 1).

**Scheme 1** Synthetic route of (*E*)-1,2-di-(3-alkylthiophene)vinylene**Scheme 2** Synthetic route of (*E*)-1,2-di-(3-bithienyl)vinylene**5-formyl-2,2'-bithiophene (4a)**

To a two-neck round bottom flask were added 6 g (36 mmol) 2,2'-bithiophene, 3 mL DMF (40 mmol), and 15 mL of 1,2-dichloroethane under argon atmosphere. Subsequently, 3.8 mL (40 mmol) of phosphorus oxychloride were added, at 0 °C. The solution was gradually brought to room temperature and allowed to reflux overnight. Afterward, the solution was cooled to room temperature and hydrolyzed with 100 mL of aqueous 1 M sodium acetate solution. Then, the mixture was extracted with dichloromethane and washed with water until neutral pH. Finally, the organic layer was dried with anhydrous magnesium sulfate for 3 h, filtered and concentrated by rotary evaporator. The title compound was purified by a silica column chromatography using hexane as eluant.

Yield 5.32 g., 76%, mp: 57–58 °C.

<sup>1</sup>H-NMR (400 MHz, CDCl<sub>3</sub>): δ(ppm) 9.85 (s, 1H); 7.67 (d, 1H); 7.35 (d, 2H); 7.24 (d, 1H); 7.07 (t, 1H).

<sup>13</sup>C-NMR: (CDCl<sub>3</sub>, 400 MHz); δ(ppm) 182.7; 147.34; 141.9; 137.5; 136.2; 128.6; 127.3; 126.3; 124.5.

**(*E*)-1,2-bis-[2,2'-bithiophene] vinylene (4b)**

To a three-neck round bottom flask were added 1.9 g (9.31 mmol) of 5-formyl-2,2'-bithiophene, and 40 mL of anhydrous THF, the solution was cooled at –18 °C under argon atmosphere and 3.3 mL (30 mmol) of titanium tetrachloride were dropwise added. The mixture was stirred during 1 h maintaining temperature at –18 °C. Afterward, to this mixture were added 4 g of Zn powder (1 g every 5 min) and stirring was maintained for half an hour at –18 °C, then allowed to gradually reach room temperature and heated for 4 h under reflux. After this time, 50 mL of 10% solution of Na<sub>2</sub>CO<sub>3</sub> (cold) and the mixture was washed with distilled water until neutral pH. Finally, the reaction mixture was extracted with dichloromethane and

washed with distilled water, dried over magnesium sulfate during 3 h. The compound was purified by continuous extraction in Soxhlet with dichloromethane and recrystallized in the same solvent.

Yield 2.3 g, 82%, mp: >220 °C (d).

<sup>1</sup>H-NMR (400 MHz, CDCl<sub>3</sub>) δ(ppm) 7.26 (s, 2H), 7.22 (dd, *J* = 5.1, 1.3 Hz, 2H), 7.18 (dd, *J* = 3.5, 1.2 Hz, 2H), 7.07 (d, *J* = 3.7 Hz, 2H), 7.02 (dd, *J* = 5.1, 3.6 Hz, 2H), 6.97–6.91 (m, 2H).

<sup>13</sup>C-NMR: (CDCl<sub>3</sub>, 400 MHz); δ(ppm) 141.5; 137.7; 136.5; 128.1; 127.4; 124.8; 124.4; 124.0; 121.5 (Scheme 2).

**References**

- Sing TB, Sariciftci NS, Jaiswal M, Menon R (2008) In: Nalva HS (ed) Handbook of organic electronics and photonics, vol 3. American Scientific Publisher, Valencia
- Fu Y, Cheng H, Elsenbaumer RL (1997) Chem Mater 9:1720–1724
- Dimitrakopoulos CD, Malenfant PRL (2002) Adv Mater 14:99–117
- Zaumseil J, Sirringhaus H (2007) Chem Rev 107:1296–1323
- Elandaloussi EH, Frère P, Richomme P, Orduna J, Garin J, Roncali J (1997) J Am Chem Soc 119:10774–10784
- Yamada S, Tokito S, Tsuisui T, Saito S (1987) J Chem Soc Chem Commun 1448
- Barker J (1989) Synth Met 32:43
- Eckhardt H, Shacklette LW, Jen KY, Crone B, Dodabalapur A, Lin YY, Filas RW, Bao Z, LaDuca A, Sarpeshkar R, Katz HE, Li W (2000) Nature 403:521–523
- Crone B, Dodabalapur A, Gelperin A, Torsi L, Katz HE, Lovinger AJ, Bao Z (2001) Appl Phys Lett 78:2229–2231
- Someya T, Katz HE, Gelperin A, Lovinger AJ, Dodabalapur A (2002) Appl Phys Lett 81:3079–3081
- Elsenbaumer RLJ (1989) Chem Phys 91:1303
- Roncali J (2000) Acc Chem Res 33:147–156
- Fuchigami H, Tsumura A, Koezuka H (1993) Appl Phys Lett 63:1372–1374
- Roncali J (1992) Chem Rev 92:711

15. Gustavson T, Bányász Á, Lazzarotto E, Markovitsi D, Scalmani G, Frisch MJ, Barone V, Impronta R (2006) *J Am Chem Soc* 128:607–619
16. Martínez F, Neculqueo G, Vásquez SO, Letelier R, Garland MT, Ibañez A, Bernede JC (2010) *J Mol Struct* 973(1–3):56–61
17. Frisch MJ, Trucks GW, Schlegel HB, Scuseria GE, Robb MA, Cheeseman JR, Jr. Montgomery JA, Vreven T, Kudin KN, Burant JC, Millam JM, Iyengar SS, Tomasi J, Barone V, Mennucci B, Cossi M, Scalmani G, Rega N, Petersson GA, Nakatsuji H, Hada M, Ehara M, Toyota K, Fukuda R, Hasegawa J, Ishida M, Nakajima T, Honda Y, Kitao O, Nakai H, Klene M, Li X, Knox JE, Hratchian HP, Cross JB, Adamo C, Jaramillo J, Gomperts R, Stratmann RE, Yazyev O, Austin AJ, Cammi R, Pomelli C, Ochterski JW, Ayala PY, Morokuma K, Voth GA, Salvador P, Dannenberg JJ, Zakrzewski VG, Dapprich S, Daniels AD, Strain MC, Farkas O, Malick DK, Rabuck AD, Raghavachari K, Foresman JB, Ortiz JV, Cui Q, Baboul AG, Clifford S, Cioslowski J, Stefanov BB, Liu G, Liashenko A, Piskorz P, Komaromi I, Martin RL, Fox DJ, Keith T, Al-Laham MA, Peng CY, Anayakkara AN, Challacombe M, Gilí PMW, Johnson B, Chen W, Wong MW, González C, Pople JA (2003) Gaussian, Inc., Gaussian 03, Revisión B.05, Pittsburgh PA
18. Chakraborty A, Kar S, Nath DN, Guchhait N (2006) *J Phys Chem A* 110:12089–12095
19. Martínez F, Voelkel R, Naegele D, Naarmann H (1989) *Mol Cryst Liq Cryst* 167:227
20. Nakayama J, Fujimiri T (1991) *Heterocycles* 32:991–1002
21. Vásquez SO (2008) *Phys Chem Chem Phys* 10(35):5459–5468
22. Meng S, Jiang J, Wang Y, Ma J (2009) *J Phys Org Chem* 22: 670–679
23. Diliën H, Marin L, Botek E, Champagne B, Lemaur V, Beljonne D, Lazzaroni R, Cleij TJ, Maes W, Lutsen L, Vanderzande D, Adriensens PJJ (2011) *Phys Chem B* 115:12040–12050
24. Tamao K, Odama S, Nakashima I, Kumada M, Minato A, Suzuki K (1982) *Tetrahedron* 38:3347–3354
25. Martínez M, Reynolds JR, Basak S, Black DA, Marynick DS, Pomerantz M (1988) *J Polym Sci Part B Polym Phys* 26:911–920